

Efficient Simulation of Wave Propagation with Implicit Finite Difference Schemes

Wensheng Zhang^{1*}, Li Tong¹ and Eric T. Chung²

¹ LSEC, Institute of Computational Mathematics and Scientific/Engineering Computing, Academy of Mathematics and Systems Science, Chinese Academy of Sciences, Beijing P. O. Box 2719, 100190 China.

² Department of Mathematics, The Chinese University of Hong Kong, Hong Kong.

Received 1 September 2010; Accepted (in revised version) 16 March 2011

Available online 27 March 2012

Abstract. Finite difference method is an important methodology in the approximation of waves. In this paper, we will study two implicit finite difference schemes for the simulation of waves. They are the weighted alternating direction implicit (ADI) scheme and the locally one-dimensional (LOD) scheme. The approximation errors, stability conditions, and dispersion relations for both schemes are investigated. Our analysis shows that the LOD implicit scheme has less dispersion error than that of the ADI scheme. Moreover, the unconditional stability for both schemes with arbitrary spatial accuracy is established for the first time. In order to improve computational efficiency, numerical algorithms based on message passing interface (MPI) are implemented. Numerical examples of wave propagation in a three-layer model and a standard complex model are presented. Our analysis and comparisons show that both ADI and LOD schemes are able to efficiently and accurately simulate wave propagation in complex media.

AMS subject classifications: 35L05, 65M06, 765Y05

Key words: Acoustic wave equation, implicit schemes, ADI, LOD, stability condition, dispersion curve, MPI parallel computations.

1. Introduction

A basic and yet important problem in geophysical exploration is to determine the response to the excitation of an impulsive source. This step involves the numerical solution of the wave equation. In seismic exploration and imaging, modeling of wave mechanisms by the acoustic wave equation is accurate and widely used (Claerbout, 1985). There are four important techniques for the simulation of wave propagation: the finite element method (Ciarlet, 1978; Cohen, *et al.*, 2001), the discontinuous Galerkin method (Chung, *et al.*,

*Corresponding author. *Email addresses:* zws@lsec.cc.ac.cn (W. Zhang), tongli@lsec.cc.ac.cn (L. Tong), tschung@math.cuhk.edu.hk (Eric T. Chung)

2006,2009), the Fourier method (Fornberg, 1975,1990; Orszag 1980; Gazdag, 1981), and the finite difference method. In this paper, we will study the finite difference method.

The simulation of waves by the finite difference method was introduced as early as 1974 by Alford (Alford, 1974). Since then, many authors have made contributions to this direction, to list a few, Bayliss, 1986; Fornberg, 1990; Levander, 1988; Marfurt, 1984; Virieux, 1984, 1986; Sei, 1995; Minkoff, 2002. Among them, the staggered-grid finite difference method has become the most popular method for acoustic or elastic wave simulation. The staggered-grid finite difference method, which solves the velocity and stress simultaneously, is an explicit scheme proposed by Virieux in 1984 (Virieux, 1984). It has several advantages for seismic exploration modeling (Levander, 1988): (1) It is stable for all values of Poisson's ratio. Thus it is ideal for problems in which the materials concerned have high Poisson's ratio. (2) It has relatively small grid dispersion and grid anisotropy, and is relatively insensitive to Poisson's ratio. (3) It can easily incorporate with the free-surface boundary conditions. The dispersion relation and stability condition of the staggered-grid schemes are given by Sei (Sei, 1995). Fornberg compared the accuracy of high-order staggered-grid finite difference scheme with the pseudospectral method (Fornberg, 1988). In general, explicit finite difference schemes have good computational efficiency, however, they are only conditionally stable.

Contrary to explicit schemes, implicit schemes are not very popular in the simulation of wave propagation due to the fact that implicit schemes typically have lower computational efficiency. In particular, at each time step, an implicit scheme requires the solution of large linear systems. While these linear systems are diagonal or banded with small bandwidth for problems in one spatial dimension, they are neither diagonal nor narrow-banded for problems in higher spatial dimensions. Hence solving them requires significant amount of computational time. However, implicit schemes still attract some attention due to their unconditional stability. Using the splitting technique, which is commonly used for parabolic problems (Thomas 1995), we may split the two (or three) dimensional problem into several one dimensional problems. Therefore, we only need to invert banded linear systems with small bandwidth.

It is our main goal in this paper to investigate this approach for enhancing efficiency of implicit schemes. We will consider two implicit schemes, the alternating direction implicit (ADI) scheme and the locally one dimensional (LOD) scheme (Fairweather and Mitchell, 1965; Samarskii, 1964). Our aims are the investigation of the error bounds, stability conditions, and dispersion curves of ADI and LOD. Moreover, we will apply a spatial parallel scheme for the numerical computations with the message passing interface (MPI). Numerical tests for a three-layer model and the benchmark Marmousi model are performed. Our results demonstrate that the wave propagation phenomena are simulated accurately by the ADI and LOD schemes.

The paper is organized as follows. The error analysis and unconditional stability for ADI and LOD schemes with arbitrary spatial accuracy are established in Sections 2 and 3 respectively. In Section 4, dispersion analysis and curves both for ADI and LOD schemes are given. In Section 5, we present accuracy comparisons of ADI and LOD schemes. In Section 6, parallel computations based on MPI environment for a three-layer model and

Marmousi model are implemented. Finally, we give conclusions in Section 7.

2. ADI scheme

The acoustic wave equation in two dimensions can be written as

$$\frac{\partial^2 u}{\partial t^2} = K \left[\frac{\partial}{\partial x} \left(\frac{1}{\rho} \frac{\partial u}{\partial x} \right) + \frac{\partial}{\partial y} \left(\frac{1}{\rho} \frac{\partial u}{\partial y} \right) \right], \quad (2.1)$$

where the bulk modulus K is the product of the velocity v squared times the density ρ

$$K = \rho v^2. \quad (2.2)$$

If the density ρ is smooth, which is the case usually adopted in seismic exploration (Claerbout, 1985), Eq. (2.1) can be simplified as

$$\frac{1}{v^2} \frac{\partial^2 u}{\partial t^2} = \frac{\partial^2 u}{\partial x^2} + \frac{\partial^2 u}{\partial y^2}, \quad (2.3)$$

where t denotes time, x and y are space variables, $u(t, x, y)$ is the acoustic pressure and $v(x, y)$ is the propagation velocity.

Let $u_{j,k}^l$ be the approximation of the exact solution u in (2.3) at the spatial grid point with indices (j, k) and time level with index l . Following standard finite difference methodology, we will express the values of second derivatives, such as $\partial^2 u / \partial x^2$, in terms of weighted sums of values of $u_{i,k}^l$ about a grid point. In particular, the approximation of $\partial^2 u / \partial x^2$ at the grid point (j, k) to the $2M$ -th order can be written as

$$\frac{\partial^2 u}{\partial x^2} = \frac{1}{\Delta x^2} \sum_{m=-M}^M \alpha_m u_{j+m,k}^l, \quad (2.4)$$

where the coefficients α_m , $m = -M, -(M-1), \dots, M-1, M$, are independent of u . It is well known that for the second-order approximation, $M = 1$ and α_m is given by

$$(\alpha_{-1}, \alpha_0, \alpha_1) = (1, -2, 1).$$

For the fourth-order approximation, $M = 2$ and α_m is given by

$$(\alpha_{-2}, \alpha_{-1}, \alpha_0, \alpha_1, \alpha_2) = \frac{1}{12}(-1, 16, -30, 16, -1).$$

For the sixth-order approximation, $M = 3$ and α_m is given by

$$(\alpha_{-3}, \alpha_{-2}, \alpha_{-1}, \alpha_0, \alpha_1, \alpha_2, \alpha_3) = \frac{1}{180}(2, -27, 270, -490, 270, -27, 2).$$

Similarly, for $\partial^2 u / \partial y^2$, we have the following order $2N$ approximation formula

$$\frac{\partial^2 u}{\partial y^2} = \frac{1}{\Delta y^2} \sum_{n=-N}^N \beta_n u_{j,k+n}^l \quad (2.5)$$

at the grid point (j, k) , where the coefficients β_n , $n = -N, -(N - 1), \dots, N - 1, N$, are independent of u . To emphasize the effect of M in α_m , we write α_m as α_m^M in appropriate places. Similarly, we write β_n^N instead of β_n to emphasize the dependence on N . Because of symmetry reason, we have $\alpha_m^M = \beta_m^M$.

Lemma 2.1. *In general, the difference coefficients α_m^M ($m = 0, 1, \dots, M$) in Eq. (2.4) is given by the following expressions:*

$$\alpha_0^M = -2 \sum_{m=1}^M \frac{1}{m^2}, \tag{2.6}$$

$$\alpha_m^M = \frac{2(-1)^{m-1}}{m^2} \frac{C_m^M}{C_m^{M+m}}, \quad m = 1, \dots, M. \tag{2.7}$$

where

$$C_m^M = \frac{M!}{(M - m)!}. \tag{2.8}$$

Proof. For consistency reasons, the coefficients α_m^M satisfy

$$\alpha_0^M + 2 \sum_{m=1}^M \alpha_m^M = 0. \tag{2.9}$$

Since the formula (2.4) is $2M$ -th order accurate, we require

$$\sum_{m=1}^M \alpha_m^M m^2 = 1, \quad \sum_{m=1}^M \alpha_m^M m^{2s} = 0, \quad s = 2, \dots, M. \tag{2.10}$$

Writing (2.9) and (2.10) in matrix-vector form, we have

$$\begin{pmatrix} 1 & 2 & 2 & \cdots & 2 & 2 & 2 \\ 0 & 1 & 2^2 & \cdots & (M - 2)^2 & (M - 1)^2 & M^2 \\ 0 & 1 & 2^4 & \cdots & (M - 2)^4 & (M - 1)^4 & M^4 \\ \cdots & \cdots & \cdots & \cdots & \cdots & \cdots & \cdots \\ 0 & 1 & 2^{2M} & \cdots & (M - 2)^{2M} & (M - 1)^{2M} & M^{2M} \end{pmatrix} \begin{pmatrix} \alpha_0^M \\ \alpha_1^M \\ \vdots \\ \alpha_M^M \end{pmatrix} = \begin{pmatrix} 0 \\ 1 \\ 0 \\ \vdots \\ 0 \end{pmatrix}. \tag{2.11}$$

By using the Gram's criterion and the properties of Vandermonde determinant, we obtain

$$\alpha_0^M = -2 \sum_{m=1}^M \frac{1}{m^2}, \tag{2.12}$$

$$\begin{aligned} \alpha_m^M &= \frac{(-1)^{m-1}}{m^2} \frac{\prod_{1 \leq i \leq M, i \neq m} i^2}{\prod_{1 \leq j < m} (m^2 - j^2) \prod_{m < j \leq M} (j^2 - m^2)} = \frac{2(-1)^{m-1}}{(M - m)!(M + m)!} \prod_{1 \leq i \leq M, i \neq m} i^2 \\ &= \frac{2(-1)^{m-1}(M!)^2}{m^2(M - m)!(M + m)!} = \frac{2(-1)^{m-1}}{m^2} \frac{C_m^M}{C_m^{M+m}}, \quad m = 1, \dots, M, \end{aligned} \tag{2.13}$$

which are the expressions (2.6) and (2.7). \square

Now we consider the following weighted ADI scheme

$$\begin{aligned} \tilde{u}_{j,k}^{l+1} - 2u_{j,k}^l + u_{j,k}^{l-1} = r_x^2 \sum_{m=-M}^M \alpha_m \left[\theta \tilde{u}_{j+m,k}^{l+1} + (1-2\theta)u_{j+m,k}^l + \theta u_{j+m,k}^{l-1} \right] \\ + r_y^2 \sum_{n=-N}^N \beta_n \left[(1-2\theta)u_{j,k+n}^l + 2\theta u_{j,k+n}^{l-1} \right], \end{aligned} \quad (2.14)$$

$$u_{j,k}^{l+1} = \tilde{u}_{j,k}^{l+1} + \theta r_y^2 \sum_{n=-N}^N \beta_n (u_{j,k+n}^{l+1} - u_{j,k+n}^{l-1}), \quad (2.15)$$

where $0 \leq \theta \leq 1$ is a weight coefficient, Δx and Δy are the spatial mesh sizes in x and y directions respectively, Δt is the time step and

$$r_x = \frac{v\Delta t}{\Delta x}, \quad r_y = \frac{v\Delta t}{\Delta y}, \quad u_{j,k}^l = u(l\Delta t, j\Delta x, k\Delta y). \quad (2.16)$$

Eqs. (2.14) and (2.15) can be written in the form

$$\begin{aligned} \left(1 - \theta r_x^2 \sum_{m=-M}^M \alpha_m \right) \tilde{u}_{j+m,k}^{l+1} = 2u_{j,k}^l - u_{j,k}^{l-1} + r_x^2 \sum_{m=-M}^M \alpha_m \left[(1-2\theta)u_{j+m,k}^l + \theta u_{j+m,k}^{l-1} \right] \\ + r_y^2 \sum_{n=-N}^N \beta_n \left[(1-2\theta)u_{j,k+n}^l + 2\theta u_{j,k+n}^{l-1} \right] \end{aligned} \quad (2.17)$$

$$\left(1 - \theta r_y^2 \sum_{n=-N}^N \beta_n \right) u_{j,k+n}^{l+1} = \tilde{u}_{j,k}^{l+1} - \theta r_y^2 \sum_{n=-N}^N \beta_n u_{j,k+n}^{l-1}, \quad (2.18)$$

where each equation has three unknown values on the left-hand side. Thus, at each time step, Eq. (2.14) or (2.17) is solved first for the x direction and then Eq. (2.15) or (2.18) is solved for the y direction. Both calculations involve only the solution of tridiagonal systems of equations. If the wavefield \tilde{u}^{l+1} is eliminated, we obtain

$$\begin{aligned} u_{j,k}^{l+1} - 2u_{j,k}^l + u_{j,k}^{l-1} \\ = r_x^2 S_x \left[\theta u_{j,k}^{l+1} + (1-2\theta)u_{j,k}^l + \theta u_{j,k}^{l-1} \right] + r_y^2 S_y \left[\theta u_{j,k}^{l+1} + (1-2\theta)u_{j,k}^l + \theta u_{j,k}^{l-1} \right] \\ - r_x^2 r_y^2 \theta^2 S_x S_y \left[u_{j,k}^{l+1} - u_{j,k}^{l-1} \right], \end{aligned} \quad (2.19)$$

where S_x and S_y are two difference operators defined as

$$S_x u_{j,k}^l = \sum_{m=-M}^M \alpha_m u_{j+m,k}^l, \quad S_y u_{j,k}^l = \sum_{n=-N}^N \beta_n u_{j,k+n}^l. \quad (2.20)$$

The truncation error is $\mathcal{O}(\Delta t^2 + \Delta x^{2M} + \Delta y^{2N})$. In fact, using the relationship

$$u_{j,k}^{l+1} - 2u_{j,k}^l + u_{j,k}^{l-1} = \Delta t^2 \frac{\partial^2 u}{\partial t^2} + \frac{\Delta t^4}{12} \frac{\partial^4 u}{\partial t^4} + \mathcal{O}(\Delta t^6), \quad (2.21)$$

we have

$$\begin{aligned}
 & S_x \left[\theta u_{j,k}^{l+1} + (1 - 2\theta)u_{j,k}^l + \theta u_{j,k}^{l-1} \right] \\
 &= \sum_{m=-M}^M \alpha_m u_{j+m,k}^l + \theta \sum_{m=-M}^M \alpha_m \left(u_{j+m,k}^{l+1} - 2u_{j+m,k}^l + u_{j+m,k}^{l-1} \right) \\
 &= \left[\Delta x^2 \frac{\partial^2 u}{\partial x^2} + \mathcal{O}(\Delta^{2+2M}) + \mathcal{O}(\Delta x^{6M}) \right] + \theta \sum_{m=-M}^M \alpha_m \left[\Delta t^2 \left(\frac{\partial^2 u}{\partial t^2} \right)_{j+m,k}^l + \mathcal{O}(\Delta t^4) \right] \\
 &= \Delta x^2 \frac{\partial^2 u}{\partial x^2} + \theta \Delta t^2 \left[\Delta x^2 \frac{\partial^4 u}{\partial t^2 \partial x^2} + \mathcal{O}(\Delta x^{2+2M}) \right] + \mathcal{O}(\Delta x^{2+2M} + \Delta t^4 \Delta x^2). \tag{2.22}
 \end{aligned}$$

Analogously, we have

$$\begin{aligned}
 & S_y \left[\theta u_{j,k}^{l+1} + (1 - 2\theta)u_{j,k}^l + \theta u_{j,k}^{l-1} \right] \\
 &= \Delta y^2 \frac{\partial^2 u}{\partial y^2} + \theta \Delta t^2 \left[\Delta y^2 \frac{\partial^4 u}{\partial t^2 \partial y^2} + \mathcal{O}(\Delta y^{2+2N}) \right] + \mathcal{O}(\Delta y^{2+2N} + \Delta t^4 \Delta y^2), \tag{2.23} \\
 & S_x S_y \left(u_{j,k}^{l+1} - u_{j,l}^n \right) \\
 &= S_x S_y \left[2\Delta t \frac{\partial u}{\partial t} + \mathcal{O}(\Delta t^3) \right] \\
 &= 2\Delta t S_x S_y \left(\frac{\partial u}{\partial t} \right) + \mathcal{O}(\Delta t^3 \Delta x^2 \Delta y^2) \\
 &= 2\Delta t \left[\Delta x^2 \Delta y^2 \frac{\partial^5 u}{\partial t \partial x^2 \partial y^2} + \mathcal{O}(\Delta y^2 \Delta x^{2+2M}) + \mathcal{O}(\Delta x^2 \Delta y^{2+2N}) \right] \\
 &\quad + \mathcal{O}(\Delta t^3 \Delta x^2 \Delta y^2). \tag{2.24}
 \end{aligned}$$

Therefore, inserting expressions (2.20)–(2.24) into Eq. (2.19), we have

$$\frac{1}{v^2} \frac{\partial^2 u}{\partial t^2} + \mathcal{O}(\Delta t^2) - \left(\frac{\partial^2 u}{\partial x^2} + \frac{\partial^2 u}{\partial y^2} \right) + \mathcal{O}(\Delta x^{2M} + \Delta y^{2N}) = 0 \tag{2.25}$$

which shows that the truncation error of the weighted ADI scheme is second-order accurate in time and $\mathcal{O}(\Delta x^{2M} + \Delta y^{2N})$ order accurate in space.

Before we prove the stability condition of the ADI implicit scheme, we first prove the following theorem.

Theorem 2.1. *The following inequality*

$$\sum_{m=-M}^M \alpha_m^M e^{im\theta} \leq 0 \tag{2.26}$$

is always true, where θ is any real number, M is any positive integer and α_m^M is the difference coefficients defined in Eqs. (2.6) and (2.7).

Proof. It can be verified that the coefficients α_m^M have the following properties:

1°

$$|\alpha_m^M| = \left| \frac{2(-1)^{m-1} C_m^M}{m^2 C_m^{M+m}} \right| \leq \frac{2}{m^2}, \quad m = 1, \dots, M. \quad (2.27)$$

2° For a fixed M , the sequence $\{\alpha_m^M\}$ ($1 \leq m \leq M$) is an alternating series and $\alpha_1^M > 0$.

3° Note that

$$|\alpha_m^M| > |\alpha_{m+1}^M|, \quad m = 1, \dots, M-1. \quad (2.28)$$

$$|\alpha_m^{M+1}| > |\alpha_m^M|, \quad m = 1, \dots, M. \quad (2.29)$$

We observe that the required expression (2.26) is equivalent to

$$\alpha_0^M + 2 \sum_{m=1}^M \alpha_m^M \cos m\theta \leq 0, \quad \theta \in \mathbb{R}. \quad (2.30)$$

Using the periodicity of $\cos m\theta$, we only need to consider $\theta \in [0, 2\pi]$. Let

$$f(\theta) = \alpha_0^M + 2 \sum_{m=1}^M \alpha_m^M \cos m\theta. \quad (2.31)$$

Then it is obvious that $f(0) = f(2\pi) = 0$ for consistency reason. Furthermore, using the property 2° we have

$$f(\pi) = \alpha_0^M + 2 \sum_{m=1}^M \alpha_m^M (-1)^m < 0. \quad (2.32)$$

Notice that

$$f'(\theta) = -2 \sum_{m=1}^M \alpha_m^M m \sin m\theta, \quad f'(\pi) = 0. \quad (2.33)$$

Thus we need to prove

$$f'(\theta) < 0, \quad \forall \theta \in (0, \pi). \quad (2.34)$$

As

$$\lim_{\theta \rightarrow 0^+} f'(\theta) = -2 \sum_{m=1}^M \alpha_m^M m^2 \theta = -2\theta < 0 \quad (2.35)$$

and $f'(\theta)$ is continuous in the interval $(0, \pi)$, proving the expression (2.34) is equivalent to proofing

$$f'(\theta) \neq 0, \quad \forall \theta \in (0, \pi). \quad (2.36)$$

We will prove this by contradiction as follows.

Suppose $\exists \theta \in (0, \pi)$ with $f'(\theta) = 0$. Let $\theta_1^{(1)} \in (0, \pi)$ and

$$f'(\theta_i^{(1)}) = 0, \quad i = 1.$$

where the superscript of θ_i is only an index for different θ_i . Using the fact that $f'(0) = f'(\pi) = 0$, we conclude by the Rolle's theorem that there exist $\theta_1^{(2)}, \theta_2^{(2)} \in (0, \pi)$ such that

$$f''(\theta_i^{(2)}) = 0, \quad i = 1, 2.$$

Thus $\exists \theta_1^{(3)} \in (0, \pi)$ with

$$f^{(3)}(\theta_i^{(3)}) = 0, \quad i = 1.$$

Using the relation $f^{(3)}(0) = f^{(3)}(\pi) = 0$, we conclude that there exist $\theta_1^{(4)}, \theta_2^{(4)} \in (0, \pi)$ such that

$$f^{(4)}(\theta_i^{(4)}) = 0, \quad i = 1, 2.$$

But

$$f^{(4)}(\theta) |_{\theta=0} = 2 \sum_{m=1}^M \alpha_m^M m^4 \cos m\theta |_{\theta=0} = 0.$$

Thus there are three null points on the interval $[0, \pi]$ satisfying

$$f^{(4)}(\theta_i^{(4)}) = 0, \quad i = 1, 2, 3.$$

Iteratively applying Rolle's theorem, we have the following facts:

(1) There are $M + 1$ zero points on the interval $[0, \pi]$ satisfying

$$f^{(2M-1)}(\theta) = 0, \quad M > 1. \tag{2.37}$$

(2) There are $M + 1$ zero points on the interval $[0, \pi]$ satisfying

$$f^{(2M)}(\theta) = 0, \quad M \geq 1. \tag{2.38}$$

So $f^{(2M)}(\theta)$ has $M + 1$ zero points on the interval $[0, \pi]$. However,

$$f^{(2M)}(\theta) = 2(-1)^M \sum_{m=1}^M \alpha_m^M m^{2M} \cos m\theta$$

and $\cos m\theta$ can be expressed as (Hua, 2009)

$$\cos m\theta = \sum_{k=0}^{[m/2]} (-1)^k C_{2k}^m (1 - \cos^2 \theta)^k \cos^{m-2k} \theta := P_m(\cos \theta),$$

where $[\cdot]$ denotes the integer part of the variable, P_m is a polynomial with degree not more than m , and the coefficient of $\cos^m \theta$ is 2^{m-1} . So $f^{(2M)}(\theta)$ is a polynomial with degree less than or equal to M and has at most M roots. This contradicts with the above statement that $f^{(2M)}(\theta)$ has $M + 1$ roots on the interval $[0, \pi]$. One notes that θ and $\cos \theta$ is one-to-one in the interval $(0, \pi)$. Therefore, we conclude $f'(\theta) < 0, \forall \theta \in (0, \pi)$. Similarly, we can prove $f'(\theta) > 0, \forall \theta \in (\pi, 2\pi)$. So $f(\theta)$ attains its maximum at the end points of interval

$[0, 2\pi]$. However, $f(0) = f(2\pi) = 0$. Therefore, $f(\theta) \leq 0$. Also, from the facts above we know the equality sign is satisfied if and only if $\theta = 2k\pi \forall k \in \mathbb{Z}$. This completes proof. \square

Now we consider the stability condition of the ADI scheme (2.14)–(2.15) or equivalently the combined form (2.18). We will use the von Neumann method to analyse its stability. We consider a Fourier component of the computational error $\varepsilon_{j,k}^l$ at grid point (j, k) and time step l . For a grid with mesh sizes Δx and Δy in directions x and y respectively, the Fourier component of the computational error is given by

$$\varepsilon_{j,k}^l = G^l e^{ik_x \Delta x} e^{ik_y \Delta y}, \quad (2.39)$$

where k_x and k_y are the wave number corresponding to x and y respectively. Substituting expression (2.39) into Eq. (2.18), we obtain

$$\begin{aligned} & G^{l+1} - 2G^l + G^{l-1} \\ &= \left[r_x^2 \sum_{m=-M}^M \alpha_m e^{imk_x \Delta x} + r_y^2 \sum_{n=-N}^N \beta_n e^{ink_y \Delta y} \right] \left[\theta G^{l+1} + (1-2\theta)G^l + \theta G^{l-1} \right] \\ &\quad - \theta^2 r_x^2 r_y^2 \sum_{m=-M}^M \alpha_m e^{imk_x \Delta x} \sum_{n=-N}^N \beta_n e^{ink_y \Delta y} (G^{l+1} - G^{l-1}). \end{aligned} \quad (2.40)$$

Rewriting this equation into a simple form as

$$aG^{l+1} + bG^l + cG^{l-1} = 0, \quad (2.41)$$

where

$$\begin{aligned} a &= 1 - \theta r_x^2 \sum_{m=-M}^M \alpha_m e^{imk_x \Delta x} - \theta r_y^2 \sum_{n=-N}^N \beta_n e^{ink_y \Delta y} \\ &\quad + \theta^2 r_x^2 r_y^2 \sum_{m=-M}^M \alpha_m e^{imk_x \Delta x} \sum_{n=-N}^N \beta_n e^{ink_y \Delta y}, \end{aligned} \quad (2.42)$$

$$b = -2 - (1-2\theta) \left[r_x^2 \sum_{m=-M}^M \alpha_m e^{imk_x \Delta x} + r_y^2 \sum_{n=-N}^N \beta_n e^{ink_y \Delta y} \right], \quad (2.43)$$

$$\begin{aligned} c &= 1 - \theta r_x^2 \sum_{m=-M}^M \alpha_m e^{imk_x \Delta x} - \theta r_y^2 \sum_{n=-N}^N \beta_n e^{ink_y \Delta y} \\ &\quad - \theta^2 r_x^2 r_y^2 \sum_{m=-M}^M \alpha_m e^{imk_x \Delta x} \sum_{n=-N}^N \beta_n e^{ink_y \Delta y}. \end{aligned} \quad (2.44)$$

Eq. (2.41) can be used to proof a sufficient condition for stability by considering the ratio of the error amplitudes as a function of time step. Let $\gamma = G^{l+1}/G^l = G^l/G^{l-1}$ be the ratio of error amplitudes in successive iterations. Then, we can insure stability by requiring that $|\gamma| \leq 1$. We can consider the stability in terms of G by dividing Eq. (2.41) by G^{l-1} to obtain

$$\gamma^2 + \tilde{b}\gamma + \tilde{c} = 0, \quad (2.45)$$

where

$$\tilde{b} = \frac{b}{a}, \quad \tilde{c} = \frac{c}{a}. \quad (2.46)$$

Eq. (2.45) is a second-order equation with one variable. The condition $|\gamma| \leq 1$ is equivalent to the following two inequalities

$$|\tilde{c}| \leq 1, \quad |\tilde{b}| \leq 1 + \tilde{c}. \quad (2.47)$$

It is easy to check that the first inequality of (2.47) is always satisfied. Notice that a is always positive by Theorem 2.1. The second inequality can be rewritten as

$$-a - c \leq b \leq a + c. \quad (2.48)$$

The left inequality of (2.48) is

$$r_x^2 \sum_{m=-M}^M \alpha_m e^{imk_x \Delta x} + r_y^2 \sum_{n=-N}^N \beta_n e^{ink_y \Delta y} \leq 0, \quad (2.49)$$

which is always true by Theorem 2.1, and the right inequality of (2.48) is

$$\left(r_x^2 \sum_{m=-M}^M \alpha_m e^{imk_x \Delta x} + r_y^2 \sum_{n=-N}^N \beta_n e^{ink_y \Delta y} \right) (4\theta - 1) \leq 4, \quad (2.50)$$

which gives the stability condition of the ADI scheme: when $\theta \geq 1/4$, the ADI is unconditional stable while

$$r_x^2 \sum_{m=-M}^M \alpha_m e^{imk_x \Delta x} + r_y^2 \sum_{n=-N}^N \alpha_n e^{ink_y \Delta y} \leq \frac{4}{4\theta - 1}, \quad \theta < \frac{1}{4}. \quad (2.51)$$

In practical computations we usually choose $\theta = 1/2$, which means this ADI scheme has unconditional stability.

3. LOD scheme

We will use the idea of LOD method to split the Eq. (2.3). A LOD form for the 2-D wave equation is

$$\frac{1}{2} \frac{1}{v^2} \frac{\partial^2 u}{\partial t^2} = \frac{\partial^2 u}{\partial x^2}, \quad (3.1)$$

$$\frac{1}{2} \frac{1}{v^2} \frac{\partial^2 u}{\partial t^2} = \frac{\partial^2 u}{\partial y^2}. \quad (3.2)$$

At each half time step, we use the following Crank-Nicolson scheme to approximate the above equations as

$$\frac{1}{2} \frac{u_{j,k}^{l+\frac{1}{2}} - 2u_{j,k}^l + u_{j,k}^{l-\frac{1}{2}}}{(\Delta t/2)^2} = \frac{1}{2\Delta x^2} \sum_{m=-M}^M \alpha_m \left(u_{j+m,k}^{l+\frac{1}{2}} + u_{j+m,k}^{l-\frac{1}{2}} \right), \quad (3.3)$$

$$\frac{1}{2} \frac{u_{j,k}^{l+1} - 2u_{j,k}^{l+\frac{1}{2}} + u_{j,k}^l}{(\Delta t/2)^2} = \frac{1}{2\Delta y^2} \sum_{n=-N}^N \beta_n \left(u_{j,k+n}^{l+1} + u_{j,k+n}^l \right), \quad (3.4)$$

which can be written as

$$\left[\left(u_{j,k}^{l+\frac{1}{2}} + u_{j,k}^{l-\frac{1}{2}} \right) - \frac{r_x^2}{4} \sum_{m=-M}^M \alpha_m \left(u_{j+m,k}^{l+\frac{1}{2}} + u_{j+m,k}^{l-\frac{1}{2}} \right) \right] = 2u_{j,k}^l,$$

$$\left[\left(u_{j,k}^{l+1} + u_{j,k}^l \right) - \frac{r_y^2}{4} \sum_{n=-N}^N \beta_n \left(u_{j,k+n}^{l+1} + u_{j,k+n}^l \right) \right] = 2u_{j,k}^{l+\frac{1}{2}},$$

or equivalently

$$\left(1 - \frac{r_x^2}{4} S_x \right) \left(u_{j,k}^{l+\frac{1}{2}} + u_{j,k}^{l-\frac{1}{2}} \right) = 2u_{j,k}^l, \quad (3.5)$$

$$\left(1 - \frac{r_y^2}{4} S_y \right) \left(u_{j,k}^{l+1} + u_{j,k}^l \right) = 2u_{j,k}^{l+\frac{1}{2}}, \quad (3.6)$$

where $r_x = \Delta t/\Delta x$ and $r_y = \Delta t/\Delta y$. S_x and S_y are the operators defined as in (2.20).

In the following, we will analyse the truncation error of LOD scheme (3.5)–(3.6). First we rewrite the Eq. (3.6) as

$$\left(1 - \frac{r_y^2}{4} S_y \right) \left(u_{j,k}^l + u_{j,k}^{l-1} \right) = 2u_{j,k}^{l-\frac{1}{2}}. \quad (3.7)$$

Substituting Eqs. (3.6) and (3.7) into (3.5) yields

$$\left(1 - \frac{r_x^2}{4} S_x \right) \left(1 - \frac{r_y^2}{4} S_y \right) \left(u_{j,k}^{l+1} - 2u_{j,k}^l + u_{j,k}^{l-1} \right) = \left(r_x^2 S_x + r_y^2 S_y - \frac{r_x^2 r_y^2}{4} S_x S_y \right) u_{j,k}^l. \quad (3.8)$$

Using the following relationships

$$u_{j,k}^{l+1} - 2u_{j,k}^l + u_{j,k}^{l-1} = \Delta t^2 \left(\frac{\partial^2 u}{\partial t^2} \right)_{j,k}^l + \frac{\Delta t^4}{12} \left(\frac{\partial^4 u}{\partial t^4} \right)_{j,k}^l + \mathcal{O}(\Delta t^6), \quad (3.9)$$

$$\frac{r_x^2}{4} S_x \left(u_{j,k}^{l+1} - 2u_{j,k}^l + u_{j,k}^{l-1} \right) = \frac{\Delta t^2}{4} \left[\Delta t^2 \left(\frac{\partial^4 u}{\partial t^2 \partial x^2} \right)_{j,k}^l + \mathcal{O}(\Delta t^2 \Delta x^{2M}) + \mathcal{O}(\Delta t^4) \right], \quad (3.10)$$

$$\frac{r_y^2}{4} S_y \left(u_{j,k}^{l+1} - 2u_{j,k}^l + u_{j,k}^{l-1} \right) = \frac{\Delta t^2}{4} \left[\Delta t^2 \left(\frac{\partial^4 u}{\partial t^2 \partial y^2} \right)_{j,k}^l + \mathcal{O}(\Delta t^2 \Delta y^{2M}) + \mathcal{O}(\Delta t^4) \right], \quad (3.11)$$

$$r_x^2 S_x u_{j,k}^l = \Delta t^2 \left(\frac{\partial^2 u}{\partial x^2} \right)_{j,k}^l + \mathcal{O}(\Delta t^2 \Delta x^{2M}), \quad (3.12)$$

$$r_y^2 S_y u_{j,k}^l = \Delta t^2 \left(\frac{\partial^2 u}{\partial y^2} \right)_{j,k}^l + \mathcal{O}(\Delta t^2 \Delta y^{2M}), \quad (3.13)$$

$$r_x^2 r_y^2 S_x S_y u_{j,k}^l = \Delta t^4 \left(\frac{\partial^4 u}{\partial x^2 \partial y^2} \right)_{j,k}^l + \mathcal{O}(\Delta t^4 (\Delta x^{2M} + \Delta y^{2N})), \quad (3.14)$$

and substituting expressions (3.9)–(3.14) into (3.8), we obtain

$$\begin{aligned} & \Delta t^2 \left(\frac{\partial^2 u}{\partial t^2} \right)_{j,k}^l + \frac{\Delta t^4}{12} \left(\frac{\partial^4 u}{\partial t^4} \right)_{j,k}^l + \mathcal{O}(\Delta t^6) \\ & + \left[\frac{\Delta t^4}{16} \left(\frac{\partial^4 u}{\partial x^2 \partial y^2} \right) + \mathcal{O}(\Delta t^4 (\Delta x^{2M} + \Delta y^{2N})) \right] \\ & - \left[\frac{\Delta t^4}{4} \frac{\partial^4 u}{\partial t^2 \partial x^2} + \frac{\Delta t^4}{4} \frac{\partial^4 u}{\partial t^2 \partial y^2} + \mathcal{O}(\Delta t^4) + \mathcal{O}(\Delta t^4 (\Delta x^{2M} + \Delta y^{2N})) \right] \\ = & \Delta t^2 \left[\frac{\partial^2 u}{\partial x^2} + \frac{\partial^2 u}{\partial y^2} \right]_{j,k}^l + \mathcal{O}(\Delta t^2 (\Delta x^{2M} + \Delta y^{2N})) \\ & - \frac{\Delta t^4}{4} \frac{\partial^4 u}{\partial x^2 \partial y^2} + \mathcal{O}(\Delta t^4 (\Delta x^{2M} + \Delta y^{2N})), \end{aligned} \quad (3.15)$$

i.e.,

$$\begin{aligned} & \left(\frac{\partial^2 u}{\partial t^2} \right)_{j,k}^l - \left(\frac{\partial^2 u}{\partial x^2} + \frac{\partial^2 u}{\partial y^2} \right)_{j,k}^l + \mathcal{O}(\Delta t^2) \\ = & - \frac{\Delta t^2}{12} \left(\frac{\partial^4 u}{\partial t^4} \right)_{j,k}^l - \frac{\Delta t^2}{4} \left(\frac{\partial^4 u}{\partial x^2 \partial y^2} \right)_{j,k}^l \\ & + \frac{1}{4} \left[\Delta t^2 \frac{\partial^2}{\partial t^2} \left(\frac{\partial^2 u}{\partial x^2} + \frac{\partial^2 u}{\partial y^2} \right)_{j,k}^l + \mathcal{O}(\Delta t^2 (\Delta x^{2M} + \Delta y^{2N})) \right] \\ & - \frac{\Delta t^4}{16} \left(\frac{\partial^4 u}{\partial x^2 \partial y^2} \right)_{j,k}^l + \mathcal{O}(\Delta t^2) + \mathcal{O}(\Delta t^4 (\Delta x^{2M} + \Delta y^{2N})) \\ = & \mathcal{O}(\Delta x^{2M} + \Delta y^{2N}) + \mathcal{O}(\Delta t^2). \end{aligned} \quad (3.16)$$

Thus the truncation error of the LOD scheme is $\mathcal{O}(\Delta t^2 + \Delta x^{2M} + \Delta y^{2N})$.

For stability analysis, we use the Fourier analysis method. We set the error components as

$$\varepsilon_{j,k}^l = G^l e^{ik_x j \Delta x} e^{ik_y k \Delta y}. \quad (3.17)$$

One notes the error satisfies the original difference equation. Substituting (3.17) into (3.8), we obtain the following relation for amplification factor $G = V^{l+1}/V^l$:

$$a_1 G^{l+1} - (2 + b_1)G^l + a_1 G^{l-1} = 0, \quad (3.18)$$

where

$$a_1 = 1 - \frac{r_x^2}{4} \sum_{m=-M}^M \alpha_m e^{ik_x m \Delta x} - \frac{r_y^2}{4} \sum_{n=-N}^N \beta_n e^{ik_y n \Delta y} + \frac{r_x^2 r_y^2}{16} \sum_{m=-M}^M \alpha_m e^{ik_x m \Delta x} \sum_{n=-N}^N \beta_n e^{ik_y n \Delta y}, \quad (3.19)$$

$$b_1 = -\frac{r_x^2}{2} \sum_{m=-M}^M \alpha_m e^{ik_x m \Delta x} - \frac{r_y^2}{2} \sum_{n=-N}^N \beta_n e^{ik_y n \Delta y} + \frac{r_x^2 r_y^2}{8} \sum_{m=-M}^M \alpha_m e^{ik_x m \Delta x} \sum_{n=-N}^N \beta_n e^{ik_y n \Delta y}. \quad (3.20)$$

Thus the ratio $\gamma = G^{l+1}/G^l$ of the amplification factor in successive iterations satisfies

$$a_1 \gamma^2 - (2 + b_1)\gamma + a_1 = 0. \quad (3.21)$$

Round-off error will not grow and the method is stable if and only if

$$\left| \frac{2 + b_1}{a_1} \right| \leq 2 \quad (3.22)$$

which leads to the inequalities

$$-2a_1 - 2 \leq b_1 \leq 2a_1 - 2, \quad (3.23)$$

since a_1 is positive by Theorem 2.1. It can be verified that the left and right inequalities of (3.23) are always satisfied. Thus the LOD implicit scheme (3.3)–(3.4) is unconditionally stable.

4. Dispersion analysis

To analyze the dispersion properties, we consider an uniform infinite medium and a plane wave

$$u(x, y, t) = \hat{u} e^{i(k_x x + k_y y - \omega t)}. \quad (4.1)$$

Then the dispersion relation for Eq. (2.3) is

$$\omega(k_x, k_y) = \pm v \sqrt{k_x^2 + k_y^2}. \quad (4.2)$$

Now we consider the discrete dispersion relation (Thomas, 1995). It can be obtained by inserting (4.1) into the concerned difference scheme. For the ADI scheme with $\theta = 1/2$, the discrete dispersion relation is

$$\omega(k_x, k_y) = -a \tan \frac{\text{Im}[\gamma_1]}{\text{Re}[\gamma_1]}, \quad (4.3)$$

where γ_1 is given by

$$\begin{aligned}
\gamma_1 = & \left\{ 2 + (1 - 2\theta) \left(r_x^2 + r^2 \sum_{n=-N}^N \beta_n e^{ink_y \Delta y} \right) \right. \\
& \pm \left[2 + (1 - 2\theta) \left(r_x^2 \sum_{m=-M}^M \alpha_m e^{imk_x \Delta x} + r^2 \sum_{n=-N}^N \beta_n e^{ink_y \Delta y} \right)^2 \right. \\
& - 4 \left(1 - \theta r_x^2 \sum_{m=-M}^M \alpha_m e^{imk_x \Delta x} \right) \cdot \left(1 - \theta r_y^2 \sum_{n=-N}^N \beta_n e^{ink_y \Delta y} \right) \\
& \left. \left(1 - \theta r_x^2 \sum_{m=-M}^M \alpha_m e^{imk_x \Delta x} - \theta r_y^2 \sum_{n=-N}^N \beta_n e^{ink_y \Delta y} \right. \right. \\
& \left. \left. - \theta^2 r_x^2 r_y^2 \sum_{m=-M}^M \alpha_m e^{imk_x \Delta x} \sum_{n=-N}^N \beta_n e^{ink_y \Delta y} \right) \right]^{\frac{1}{2}} \left. \right\} \\
& \times \left\{ 2 \left(1 - \theta r_x^2 \sum_{m=-M}^M \alpha_m e^{imk_x \Delta x} \right) \left(1 - \theta r_y^2 \sum_{n=-N}^N \beta_n e^{ink_y \Delta y} \right) \right\}^{-1}. \quad (4.4)
\end{aligned}$$

Similarly, for the LOD implicit scheme, the discrete dispersion relation is

$$\omega(k_x, k_y) = -a \tan \frac{\text{Im}[\gamma_2]}{\text{Re}[\gamma_2]}, \quad (4.5)$$

where

$$\begin{aligned}
\gamma_2 = & \left\{ \left(\frac{r_x^2}{2} \sum_{m=-M}^M \alpha_m e^{ik_x m \Delta x} + \frac{r_y^2}{2} \sum_{n=-N}^N \beta_n e^{ik_y n \Delta y} \right. \right. \\
& \left. \left. - \frac{r_x^2 r_y^2}{8} \sum_{m=-M}^M \alpha_m e^{ik_x m \Delta x} \sum_{n=-N}^N \beta_n e^{ik_y n \Delta y} \right) \right. \\
& \pm \left[\left(\frac{r_x^2}{2} \sum_{m=-M}^M \alpha_m e^{ik_x m \Delta x} + \frac{r_y^2}{2} \sum_{n=-N}^N \beta_n e^{ik_y n \Delta y} \right. \right. \\
& \left. \left. - \frac{r_x^2 r_y^2}{8} \sum_{m=-M}^M \alpha_m e^{ik_x m \Delta x} \sum_{n=-N}^N \beta_n e^{ik_y n \Delta y} \right)^2 \right. \\
& \left. - 4 \left(1 - \frac{r_x^2}{4} \sum_{m=-M}^M \alpha_m e^{ik_x m \Delta x} \right) \left(1 - \frac{r_y^2}{4} \sum_{n=-N}^N \beta_n e^{ik_y n \Delta y} \right) \right]^{\frac{1}{2}} \left. \right\} \\
& \times \left\{ 2 \left(1 - \frac{r_x^2}{4} \sum_{m=-M}^M \alpha_m e^{ik_x m \Delta x} \right) \left(1 - \frac{r_y^2}{4} \sum_{n=-N}^N \beta_n e^{ik_y n \Delta y} \right) \right\}^{-1}. \quad (4.6)
\end{aligned}$$

In Figs. 1–4, we present the dispersion curves of the ADI and LOD implicit schemes. For simplicity, we set $\Delta x = \Delta y = h$. All the implicit schemes used here are second-order in

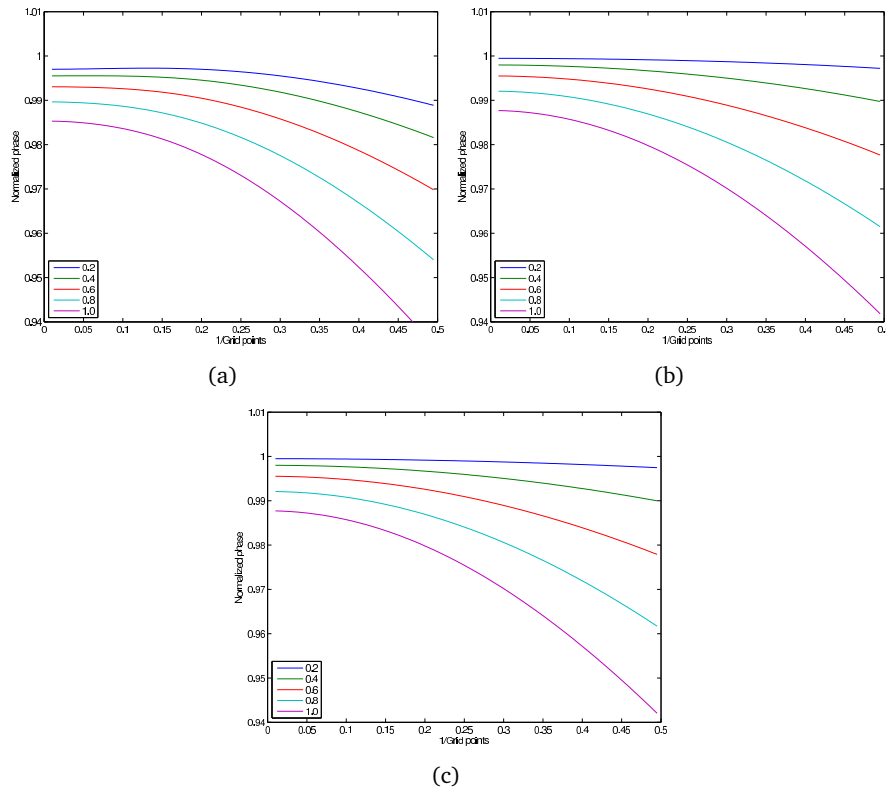


Figure 1: The dispersion curves with various CFL numbers for the (a) second-order, (b) fourth-order and (c) sixth-order ADI difference schemes.

time. The CFL number is defined by $\nu\Delta t/h$. Figs. 1(a), 1(b) and 1(c) show the dispersion curves for ADI implicit schemes ($\theta = 1/2$) with the second-order, fourth-order and sixth-order accuracy in space respectively. Five curves are shown in each figure to represent five different CFL numbers. The five CFL numbers are chosen as 0.2, 0.4, 0.6, 0.8 and 1.0. The wave number k_y in Fig. 1 is set as $\pi/4$. From Fig. 1, we see that the dispersion error increases as the CFL number grows. In Fig. 2, we set the CFL number as 1.0, and investigate the behavior of dispersion error with respect to propagation angle in the x direction. Angles in Fig. 2 are chosen as 5° , 20° , 35° , 50° and 65° . The results for the ADI scheme ($\theta = 1/2$) with a fixed CFL number are plotted in Fig. 2, and we see that the dispersion error increases as the propagation angle grows.

Figs. 3 and 4 show the dispersion curves for the LOD implicit schemes. Figs. 3(a), 3(b) and 3(c) are the curves with various CFL numbers for the second-order, fourth-order and sixth-order accurate schemes respectively. Figs. 4(a), 4(b) and 4(c) are the curves with various propagating angles in the x direction for the second-order, fourth-order and sixth-order accurate schemes respectively. The phenomena and conclusions are similar to that of the ADI implicit schemes. Fig. 3 shows that dispersion error increases as the CFL number grows. Fig. 4 shows that dispersion error increases as the propagation angle increases.

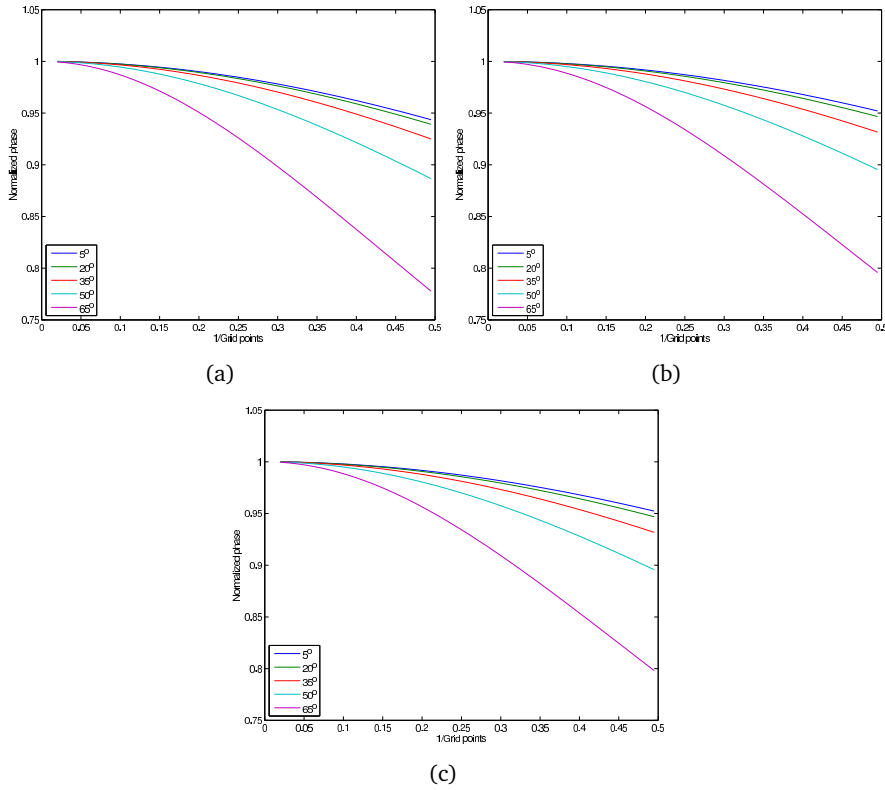


Figure 2: The dispersion curves with various propagation angles for the (a) second-order, (b) fourth-order and (c) sixth-order ADI difference schemes.

By comparing the dispersion curves above, we see that the second-order scheme has much lower accuracy than the fourth-order and sixth-order schemes. Moreover, the accuracy difference between the fourth-order and sixth-order schemes is not obvious, though the LOD scheme has a little higher accuracy than the ADI scheme.

We also provide comparisons of ADI/LOD with the standard explicit scheme. Without loss of generality, we choose a fourth-order standard explicit scheme. Fig. 5(a) demonstrates dispersion curves with various CFL numbers. Fig. 5(b) demonstrates dispersion curves with various propagating angles. Comparing Figs. 3(b) and 4(b) with 5(a) and 5(b), we see that the error of the fourth-order standard explicit scheme is slightly less than that of the fourth-order ADI/LOD schemes. The comparisons for the second-order and sixth-order schemes are similar to the fourth-order case. Therefore, we omit the details.

5. Comparisons with analytical solutions

In this section, we present accuracy comparisons of the ADI and LOD schemes. The analytical solution of Eq. (2.3) is $\sin \beta vt \sin[\beta(x+y)/\sqrt{2}]$. The solution domain is $[0, 200] \times [0, 200]$. We choose parameter $\beta = 0.6$ and $v = 100$. The boundary and initial conditions

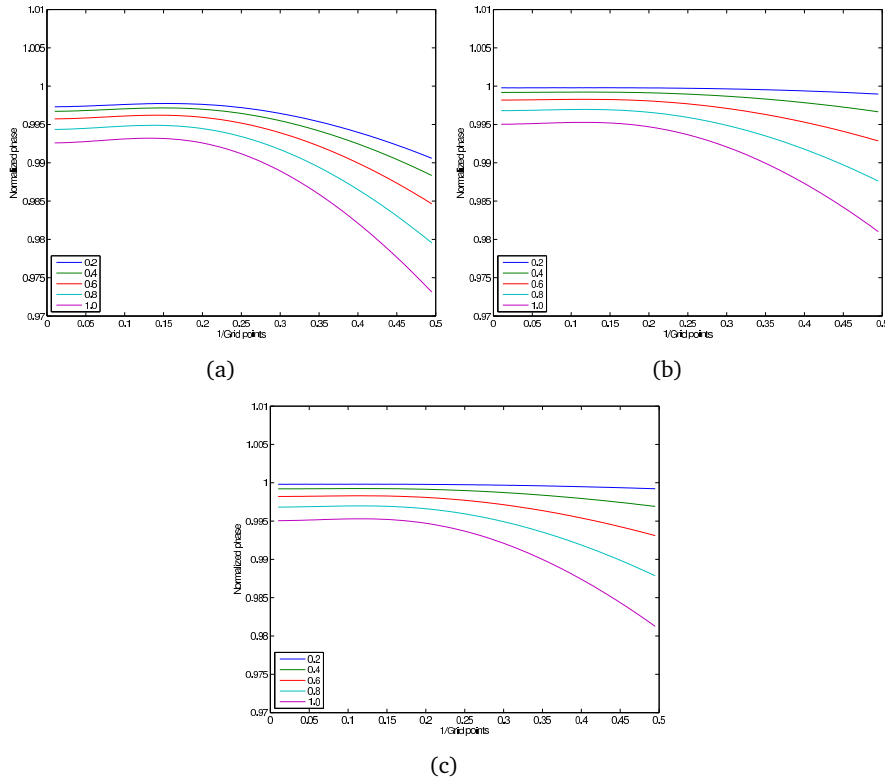


Figure 3: The dispersion curves with various CFL numbers for the (a) second-order, (b) fourth-order and (c) sixth-order LOD difference schemes.

are obtained from this analytical solution.

Fig. 6 is a comparison of wave vibration between the approximation and the exact solution at position $(x_0, y_0) = (80, 80)$. In computations we set $\Delta t = 0.001$ and $\Delta x = \Delta y = 0.005$. In Fig. 6(a), we plot the results of ADI schemes with the second-order, fourth-order and sixth-order accurate schemes respectively. The exact solution is also plotted for comparison. The results for LOD schemes are also plotted in Fig. 6(b). Tables 1 and 2 are the maximum norm and the L_2 -norm errors of ADI and LOD schemes respectively. From Fig. 5 and Tables 1 and 2, we see that the second-order scheme has much lower accuracy than that of the fourth-order and the sixth-order schemes. Both the fourth-order and sixth-order ADI/LOD schemes are able to fit the exact solution well. The fourth-order LOD scheme is a little more accurate than the fourth-order ADI scheme, and the sixth-order LOD scheme is more accurate than the sixth-order ADI scheme. However, the differences are not observable by naked eyes. In many applications, the fourth-order schemes can meet practical requirements. Finally we show the convergence order of L_2 -norm errors over different grids. To save space, we present the result of fourth-order LOD scheme. The result for different time and space steps is given in Table 3. The log-log plot for the L_2 norm errors for the fourth-order LOD scheme is shown in Fig. 7. The slope of the line is

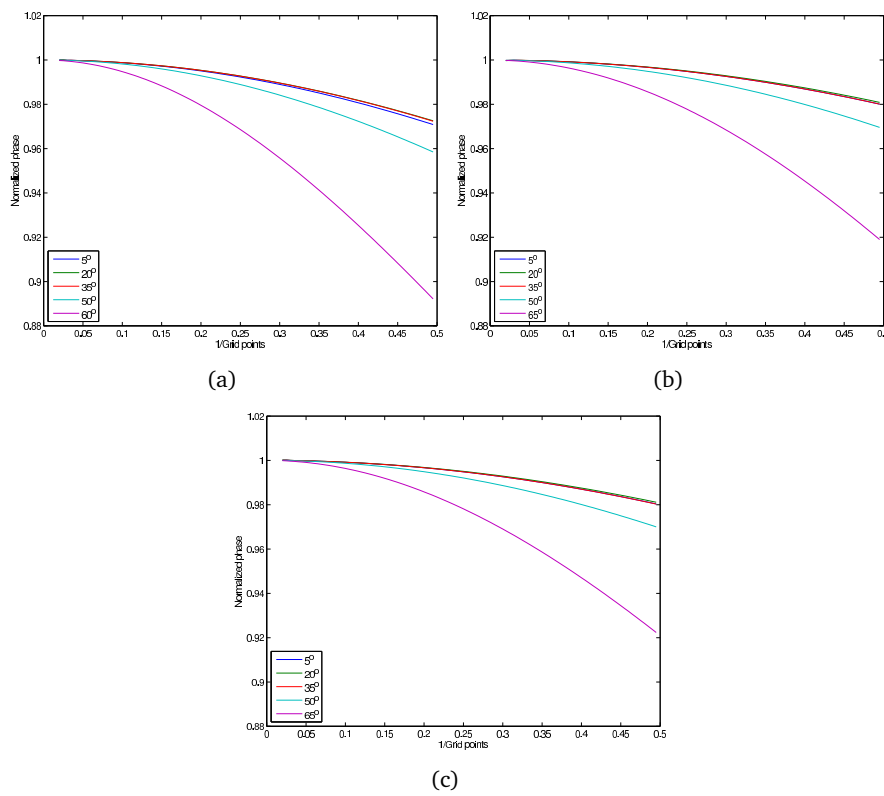


Figure 4: The dispersion curves with various propagation angles for the (a) second-order, (b) fourth-order and (c) sixth-order LOD difference schemes.

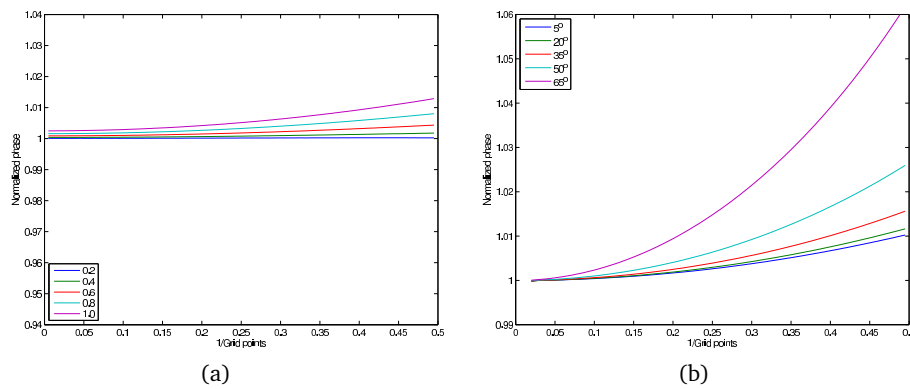


Figure 5: The dispersion curves with (a) various CFL numbers and (b) various propagating angles for the fourth-order standard explicit difference scheme.

4.70 which suggests the order of convergence of this LOD scheme is 4.70. More about the convergence order can be found in the reference of Geiser (2008).

Table 1: Maximum and L_2 norm errors for ADI schemes.

norm	ADI 2nd	ADI 4th	ADI 6th
∞ norm	0.789387	0.068770	0.019773
L_2 norm	0.136455	0.015305	0.004671

Table 2: Maximum and L_2 norm errors for LOD schemes.

norm	LOD 2nd	LOD 4th	LOD 6th
∞ norm	0.775119	0.058133	0.008514
L_2 norm	0.134237	0.013062	0.002056

Table 3: L_2 norm errors for fourth-order LOD scheme.

Δt	Δx	L_2 -norm errors
1/500	1/50	1.617492E-02
1/600	1/60	7.086813E-03
1/800	1/80	1.894149E-03
1/1000	1/100	6.114570E-04
1/1200	1/120	2.562042E-04
1/1400	1/140	1.355431E-04

6. MPI parallel computations

Generally speaking, the computational efficiency of implicit schemes is lower than that of explicit schemes. The main reason is that the implicit scheme requires the solution of a linear algebraic system at each time step. However, computational efficiency of implicit schemes can be improved by parallel algorithms. Here we adopt the spatial parallelism as it is the most efficient way to parallelize finite difference simulations. We have implemented a domain decomposition scheme by dividing the solution domain into several subdomains.

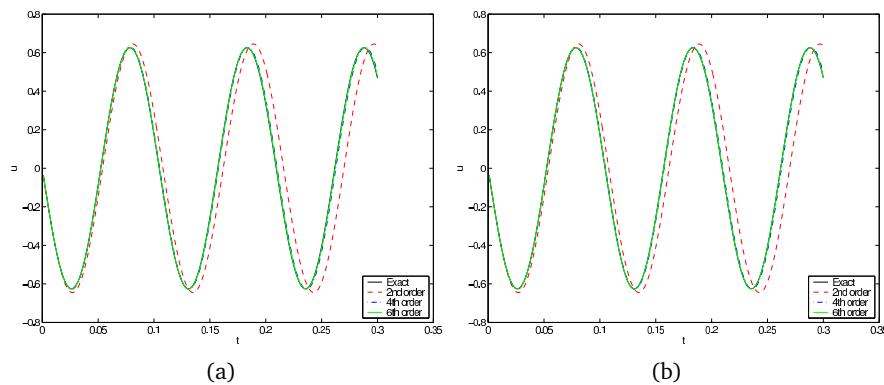


Figure 6: A comparison between numerical and exact solutions for (a) ADI scheme with the second-order, fourth-order and sixth-order spatial accuracy respectively and (b) LOD scheme with the second-order, fourth-order and sixth-order spatial accuracy respectively.

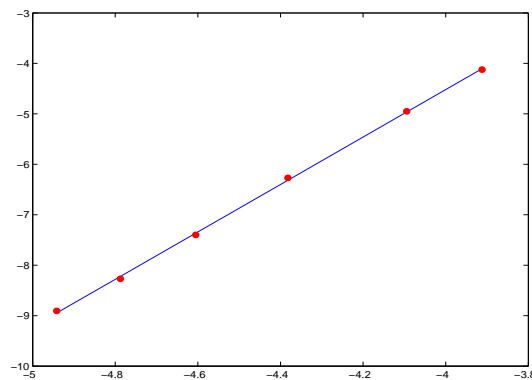


Figure 7: A log-log plot for the L_2 norm errors for the fourth-order LOD scheme.

In order to balance workload and to minimize the communication time, all the subdomains have the same size. At each time step, the wavefield data is required to exchange along the boundaries of the subdomains. The information about the neighboring grid points comes from the adjacent subdomains.

The accuracy of the wave propagation is first tested by simulating the wavefield for a three-layer model. This model is described by a 150×150 grid, and the velocities of the three layers are 1200m/s, 1500m/s and 1700m/s respectively. In computations we choose $\Delta x = \Delta z = 20\text{m}$ and $\Delta t = 0.002\text{s}$. The source position is at the center of the model, i.e., at grid point (75, 75). The source pulse is a banded Ricker wavelet with a dominant frequency of 30Hz. It is depicted by $e^{-100t^2} \sin(30t)$. The shape of Ricker wavelet may simulate a real exploration in oil geophysical exploration. Fig. 8 shows the snapshots of the acoustic propagation in this layered model. The numerical scheme used in this simulation is second-order accurate in time and fourth-order accurate in space. Fig. 8(a) shows the results computed by the ADI scheme while Fig. 8(b) shows the results obtained by the LOD

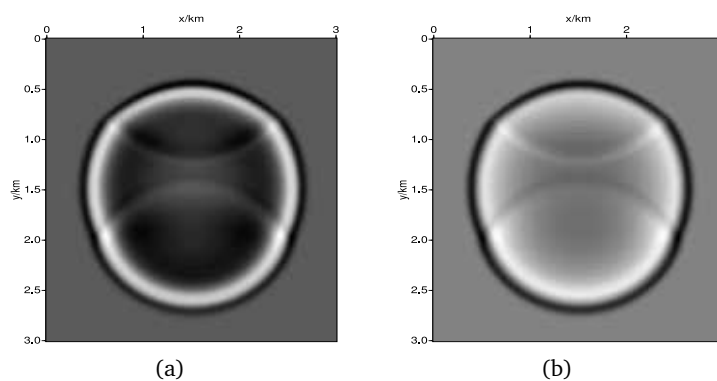


Figure 8: Wave propagation in a three-layer model simulated by (a) the ADI implicit scheme and (b) the LOD implicit scheme. Both schemes are fourth-order accurate in space.

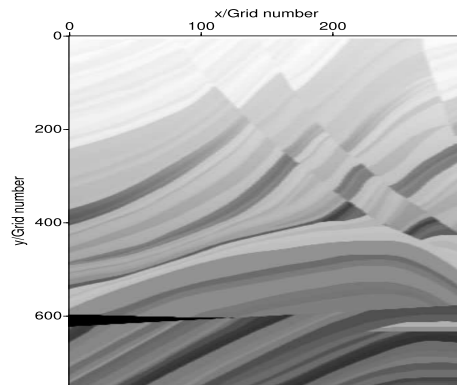


Figure 9: Marmousi velocity model.

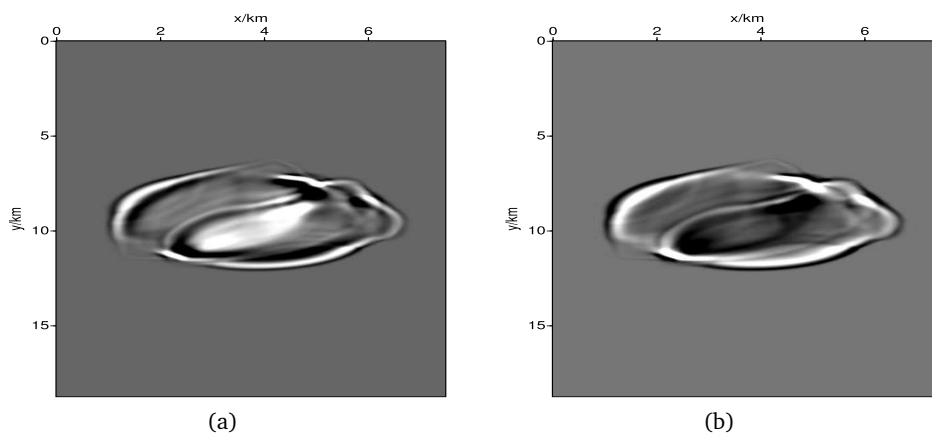


Figure 10: Wave propagation in Marmousi model simulated by (a) the ADI implicit scheme and (b) the LOD implicit scheme. Both schemes are fourth-order accurate in space.

scheme. In Fig. 8, the reflected wave and transmitted wave caused by the two interfaces are clearly observed. The wavefront is very sharp. Since the material is heterogeneous, the wavefront is not a circle.

The next model for testing our MPI algorithm is the so-called Marmousi model shown in Fig. 9. The Marmousi model is a benchmark model created by the Institut Français du Pétrole in 1988. It is widely used for testing the ability and accuracy of inversion/migration methods (cf., Zhang, *et al.*, 2000). Here we simulate the wave propagation in this model. The velocity varies from the minimum value of 1500 m/s to the maximum value of 5500 m/s, represented by grey level from white to black. We choose a grid with $N_x \times N_z = 400 \times 750$. The computational results by the fourth-order ADI and LOD schemes are shown in Fig. 10, while Fig. 11 demonstrates the results computed by the sixth-order ADI and LOD schemes. From these figures we see that the fourth-order or sixth-order ADI and LOD schemes behave similarly for this model. In addition, the wavefronts of wave propagation in the complicated media are accurately simulated, and the

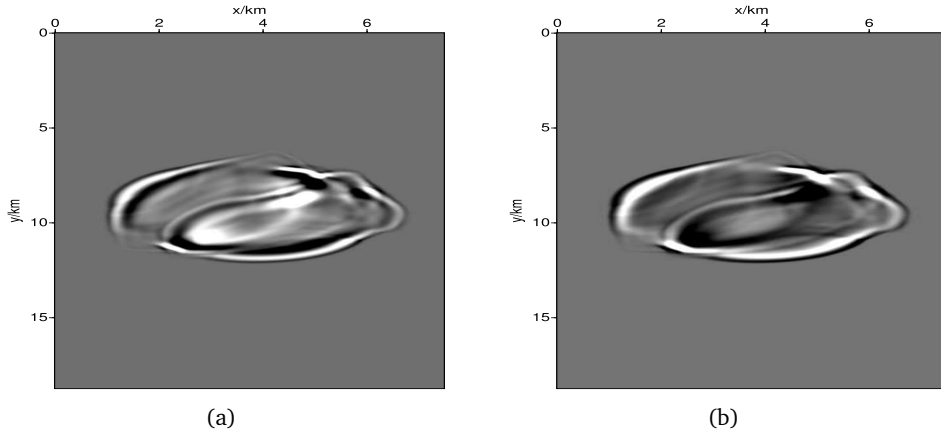


Figure 11: Wave propagation in Marmousi model simulated by (a) the ADI implicit scheme and (b) the LOD implicit scheme. Both schemes are sixth-order accurate in space.

outermost wavefront is gradually spread. We also observe the reflection waves from the inner wavefronts. As we expected, the differences between the simulating results from the ADI and LOD schemes are very small. For computational costs, the number of operations for ADI scheme (2.14)–(2.15) (with $\theta = 1/2$ and $N = M$) and (3.3)–(3.4) are $(4M + 6N)n_x n_y + 31n_x n_y - 15(n_x + n_y)$ and $4(M + N)n_x n_y + 30n_x n_y - 15(n_x + n_y)$, respectively, where n_x denotes the grid number in direction x , and n_y the grid number in direction y . For simplicity, we provide only comparisons of computational costs for the fourth-order schemes. The real computational time for the fourth-order ADI and LOD schemes are 4m1.656s and 3m55.701s, respectively, both on the same PC with 2.1Ghz. Thus the cost of LOD is slightly less than that of ADI, which is consistent with our theoretical analysis.

7. Conclusions

In this paper, parallel simulation with implicit schemes are investigated. For both ADI and LOD implicit schemes, we have analyzed their truncation error, stability conditions and dispersion curves. We proved that both the ADI scheme with $\theta \geq 1/4$ and LOD scheme are unconditionally stable for any spatial accuracy. The dispersion analysis shows that the error increases as the CFL number grows or as the propagation angle increases. For the same order accuracy in space, the LOD implicit scheme has a little less dispersion error than that of ADI. Moreover, the LOD scheme can be easily extended to the three dimensional cases than the ADI scheme. From this point of view, the LOD implicit scheme is superior. Numerical experiments are performed for a three-layer model and a standard complex model named Marmousi model. The wave propagation are clearly simulated. All computations are implemented based on the MPI environment. The results in this paper show that implicit schemes can be used to simulate wave propagation in the complex media.

Acknowledgments The authors are grateful to the anonymous referees for their careful reading and constructive comments, which have improved the paper. Thanks are also given to prof. Z. Zhang for his valuable helps. This research is supported by the State Key Project (2010CB731505), National Key Foundation Project (10431030), and Director Foundation Project of Laboratory of Scientific and Engineering Computing (LSEC).

References

- [1] R. M. ALFORD, K. R. KELLY, AND D. M. BOORE, *Accuracy of finite-difference modeling of acoustic wave equations*, *Geophysics*, 39 (1974), pp. 834–842.
- [2] A. BAYLISS, K. E. JORDAN, B. J. LEMESURIER, AND E. TURKEL, *A fourth-order accurate finite-difference scheme for the computation of elastic waves*, *Bull. Seis. Soc. Am.*, 76 (1986), pp. 1115–1132.
- [3] C. CERJAN, D. KOSLOFF, R. KOSLOFF, AND M. RESHEF, *A nonreflecting boundary condition for discrete acoustic and elastic wave equations*, *Geophysics*, 50 (1985), pp. 705–708.
- [4] E. T. CHUNG AND B. ENGQUIST, *Optimal discontinuous Galerkin methods for wave propagation*, *SIAM J. Numer. Anal.*, 44 (2006), pp. 2131–2158.
- [5] ———, *Optimal discontinuous Galerkin methods for the acoustic wave equation in higher dimensions*, *SIAM J. Numer. Anal.*, 47 (2009), pp. 3820–3848.
- [6] P. G. CIARLET, *The finite element method for elliptic problems*, North-Holland Publishing Company, Amsterdam, New York, Oxford, 1978.
- [7] J. F. CLAERBOUT, *Imaging the earth's interior*, Blackwell Scientific Publications Inc., 1982.
- [8] G. COHEN, P. JOLY, J. E. ROBERTS, AND N. TORDJMAN, *Higher order triangular finite elements with mass lumping for the wave equation*, *SIAM J. Numer. Anal.*, 38 (2001), pp. 2047–2078.
- [9] M. A. DABLAIN, *The application of higher-order differencing for the scalar wave equation*, *Geophysics*, 51 (1986), pp. 54–66.
- [10] G. FAIRWEATHER, AND A. R. MITCHELL, *A high Accuracy alternating direction method for the wave equation*, *IMA J. Appl. Math.*, 1 (1965), pp. 309–316.
- [11] B. FORNBERG, *On a Fourier method for the integration of hyperbolic equations*, *SIAM J. Numer. Anal.*, 12 (1975), pp. 509–528.
- [12] ———, *The pseudospectral method: accurate representation of interfaces in elastic wave calculations*, *Geophysics*, 53 (1988), pp. 625–637.
- [13] ———, *High-order finite differences and the pseudospectral method on staggered grids*, *SIAM J. Numer. Anal.*, 27 (1990), pp. 904–918.
- [14] J. GAZDAG, *Modeling of the acoustic wave equation with transform methods*, *Geophysics*, 46 (1981), pp. 854–859.
- [15] J. GEISER, *Higher-order splitting method for elastic wave propagation*, *International Journal of Mathematics and Mathematical Sciences*, Volume 2008, Article ID 291968, 31 pages.
- [16] J. GEISER, *Fourth-order splitting methods for time-dependent differential equations*, *Numer. Math. Theor. Meth. Appl.*, 1 (2008), pp. 321–339.
- [17] A. R. GOURLAY AND A. R. MITCHELL, *A classification of split difference methods for hyperbolic equations in several space dimensions*, *SIAM J. Numer. Anal.*, 6 (1969), pp. 62–71.
- [18] L. G. HUA, *Introduction to higher mathematics (in Chinese)*, Academic Press, Beijing, China, 2009.
- [19] K. R. KELLY, R. W. WARD, S. TREITEL, AND R. M. ALFORD, *Synthetic seismograms: A finite-difference approach*, *Geophysics*, 41 (1976), pp. 2–27.

- [20] D. D. KOSLOFF AND E. BAYSAL, *Forward modeling by a Fourier method*, *Geophysics*, 47 (1982), pp. 1402–1412.
- [21] D. KOSLOFF, D. KESSLER, A. Q. FILHO, E. TESSMER, A. BEHLE, AND R. STRAHILEVITZ, *Solution of the equations of dynamic elasticity by a Chebychev spectral method*, *Geophysics*, 55 (1990), pp. 734–748.
- [22] D. KOSLOFF, M. RESHEF, AND D. LOWENTHAL, *Elastic wave calculations by the Fourier method*, *Bull. Seis. Soc. Am.*, 74 (1984), pp. 875–891.
- [23] A. R. LEVANDER, *Fourth-order finite-difference P-SV seismograms*, *Geophysics*, 53 (1988), pp. 1425–1436.
- [24] K. J. MARFURT, *Accuracy of finite-difference and finite-element modelling of the scalar and elastic wave equations*, *Geophysics*, 49 (1984), pp. 533–549.
- [25] S. E. MINKOFF, *Spatial parallelism of a 3D finite difference velocity-stress elastic wave propagation code*, *SIAM J. Sci. Comput.*, 24 (2002), pp. 1–19.
- [26] S. A. ORSZAG, *Spectral methods for problems in complex geometries*, *J. Comput. Phys.*, 37 (1980), pp. 70–92.
- [27] A. A. SAMARSKII, *Local one-dimensional difference schemes for multi-dimensional hyperbolic equations in an arbitrary region*, *Zh. Vychisl. Mat. Mat. Fiz.*, 4 (1964), pp. 638–648.
- [28] A. SEI, *A family of numerical schemes for the computation of elastic waves*, *SIAM J. Sci. Comput.*, 16 (1995), pp. 898–916.
- [29] J. W. THOMAS, *Numerical partial differential equations: finite difference methods*, Springer-Verlag New York, Inc., 1995.
- [30] J. VIRIEUX, *SH-wave propagation in heterogeneous media: velocity-stress finite-difference method*, *Geophysics*, 49 (1984), pp. 1933–1957.
- [31] ———, *P-SV wave propagation in heterogeneous media: velocity-stress finite-difference method*, *Geophysics*, 51 (1986), pp. 889–901.
- [32] G. ZHANG AND W. ZHANG, *Parallel implementation of 2-D prestack depth migration*, *The Fourth International Conference/Exhibition on High performance Computing in Asia-Pacific Region*, Beijing, China, Expanded Abstracts, 2000, pp. 970–975.